Open Geosci. 2019; 11:572–580 **DE GRUYTER**

Research Article

გ

Liu Yaoning*, Liu Shucai, Li Maofei, Liu Xinming, and Guo Weihong

A Study on Transient Electromagnetic Interpretation Method Based on the Seismic Wave Impedance Inversion Model

https://doi.org/10.1515/geo-2019-0047 Received Jan 02, 2019; accepted Jul 16, 2019

Abstract: A comprehensive transient electromagnetic interpretation method based on seismic wave impedance inversion has been proposed according to the advantages of seismic and transient electromagnetic exploration methods to mitigate of hidden water inrush disasters in coalmines. Combined seismic wave impedance inversion results and resistivity logging data, the method was used to establish a geo-electric model. The stratigraphic horizon and the stratigraphic electrical characteristics were determined by the wave impedance inversion data and the resistivity logging data respectively. Furthermore, the structure and water-bearing property in the stratum were estimated by the analysis of the difference between the measured transient electromagnetic data and the calculated data from the forward model. The numerical calculation of the fault-containing model shows that the comprehensive interpretation method could determine the water-bearing capability of the fault as well as it tendency. An advantage of this new method is the effective avoidance of the influence of low-impedance overburden on the data interpretation. The practical application can accurately explain the location and the water-bearing property of the disaster-causing factors of the hidden water inrush in the coalmines.

Keywords: transient electromagnetic interpretation method; seismic wave impedance inversion; the disaster factors; the hidden water inrush; water-bearing property

Liu Shucai, Li Maofei, Guo Weihong: Institute of Mine Water Hazards Prevention and Controlling Technology, School of Resources and Geosciences, China University of Mining and Technology, Xuzhou, Jiangsu Province 221116, China

1 Introduction

At present, the disaster-causing factors of the hidden water inrush in coal mines are mainly detected by electromagnetic exploration, which includes the transient electromagnetic method(TEM), direct current sounding method, controllable source audio magnetotelluric method, and the high-density resistivity method. Among of them, the TEM is widely used [1-4]. A certain effect has been achieved on explaining the occurrence range of the disaster-causing source of the hidden water inrush in the coalmines by detecting the electrical differences between the disaster-causing source of the hidden water inrush and the surrounding rock in the coal mines. Due to the volume effect of the electrical exploration, some factors such as the low spatial scale precision and the strong multisolution influence the determination, it is still far from the fine detection requirements for a safe and efficient green mining in the coal mines [5, 6].

In the past decades, coalmines in China have carried out a high-precision three-dimensional seismic exploration in the mining areas and have achieved remarkable results in the detection of the small structures in the mining areas [7–9]. Based on the difference of the elastic mechanical properties of rocks, the seismic exploration technology excites and observes the transmitting rules of elastic waves in rocks for exploration. It has a high vertical and horizontal resolution and is highly sensitive in dividing strata and small structures. However, the elastic parameters of the rocks are not highly correlated with its aquosity; therefore, it is difficult to identify the stratum water-rich area by seismic exploration. The application of three-dimensional seismic in exploration of hidden water inrush hazard sources in multiple mines is not satisfactory [10, 11].

Liu Xinming: College of Mining Engineering, North China University of Science and Technology, Tangshan, Hebei Province 063000, China



^{*}Corresponding Author: Liu Yaoning: Institute of Mine Water Hazards Prevention and Controlling Technology, School of Resources and Geosciences, China University of Mining and Technology, Xuzhou, Jiangsu Province 221116, China; Email: tb14010014@cumt.edu.cn

Comprehensive interpretation combined with multiple geophysical methods is the direction and trend of the geophysical exploration development [12–15]. Based on the respective characteristics of these two methods, this paper studies whether comprehensive inversion interpretation combined with transient electromagnetic method and seismic method can be used as a new method and theoretical basis for the detailed detection of hidden water inrush hazard sources in the coalmines.

2 Method

Wave impedance inversion is a commonly used interpretation method in seismic exploration data processing. It has good resolution for stratigraphic stratification and structural location, but it cannot effectively identify the aquosity of the stratum. The TEM can reflect the difference between underground water-rich area and surrounding rock. It is a very mainstream method for detecting the aquosity in coal seam. However, there is a multi-solution for the division of the position and the location of the anomalous body due to the volume's effect of the method itself. The method in this paper is a kind of comprehensive interpretation method of transient electromagnetic based on the wave impedance inversion result model.

The method flow is shown in Figure 1: Firstly, the wave impedance inversion is carried out based on the measured three-dimensional seismic data and the density logging data in the work area to obtain the wave impedance inversion section. Then, the geoelectric model is established by combining the resistivity logging data in the work area, and the established geoelectric model is used for a transient electromagnetic forward calculation. At this time, the established geophysical model does not contain water. Finally, the measured transient electromagnetic data and forward data are combined for comprehensive analysis, thereby the comprehensive interpretation of the geological structure location and its water-bearing properties being carried out.

The comprehensive interpretation of the transient electromagnetic based on the wave impedance inversion can be used not only in further identifying the structure of the exploration area, but also effectively in discriminating the water-bearing property of the structure in the exploration area. In addition, it is often susceptible to overly low-impedance the stratum or low-impedance the anomalies in the process of transient electromagnetic detection, causing the low-impedance anomalies below to not be effectively distinguished. However, two methods based on

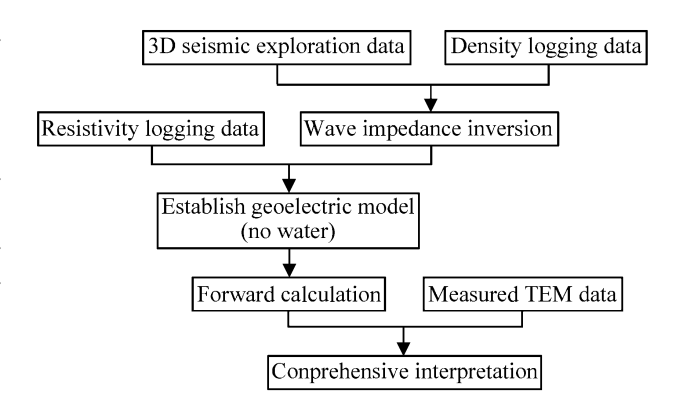


Figure 1: Flow of the Comprehensive Interpretation Method

a different physical exploration, which are used for comprehensive interpretation, can eliminate the influence of a low-impedance overburden effectively.

3 Results and Discussion

The method was analyzed and discussed by numerical simulation in this section. In order to ensure the reliability of the data, we use two methods for the forward modeling of the same model and verify the method based on the forward modeling data. Wave impedance inversion is based on forward modeling data in the paper. In the model setting, the seismic exploration method mainly considers two parameters, including stratum thickness and the compression wave velocity, while the transient electromagnetic model mainly considers the stratum thickness and resistivity.

3.1 Forward and inversion of seismic exploration

The settings of the seismic forward model is given in Figure 2. The overburden compression wave velocity is set to 1,800 m/s, the hanging side thickness 50m, and the heading side thickness 100m. The yellow layer compression wave velocity is set to 2,400m/s, the hanging and heading side thicknesses 100m. The green layer compression wave velocity is set to 3,000m/s, the hanging and heading side thicknesses 20m, as well as the thickness of the fracture zone of the fault 20m, the compression wave velocity 2,200m/s, and the perpendicular throw 50, and the compression wave velocity of the lowest stratum is set to 4,000m/s. The fault runs through all of the layers below to overburden, with the model length being in length

574 — L. Yaoning et al. DE GRUYTER

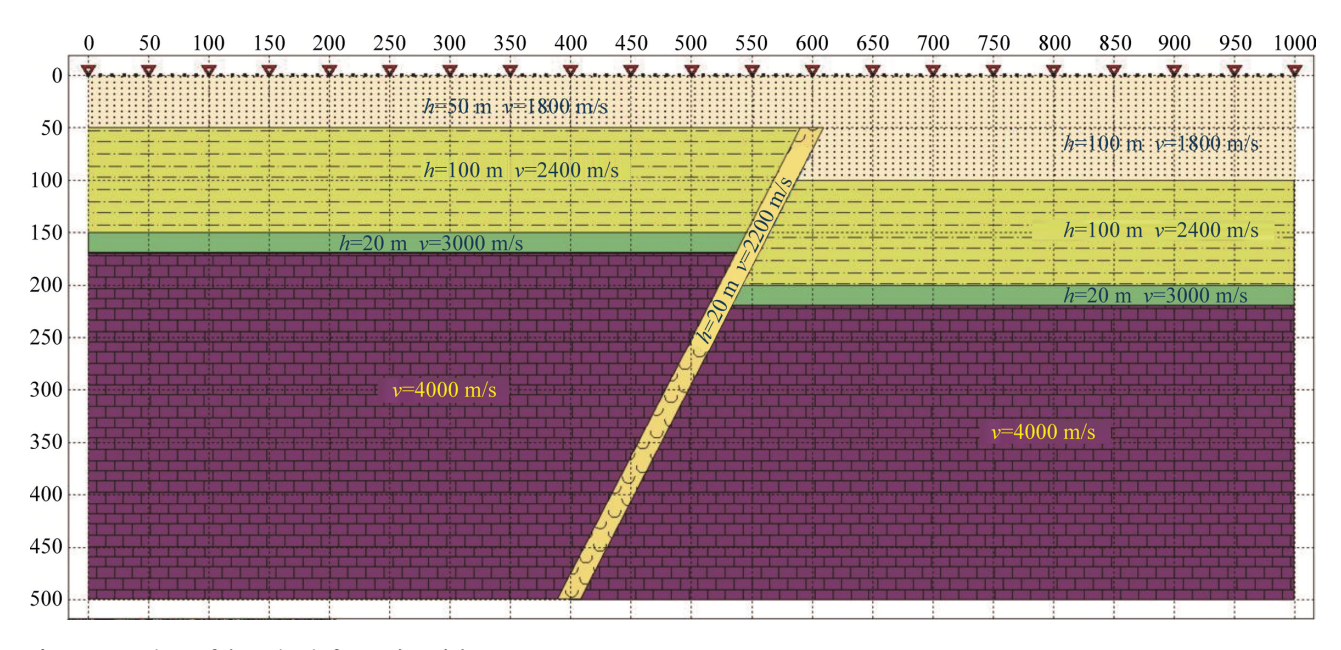


Figure 2: Settings of the seismic forward model

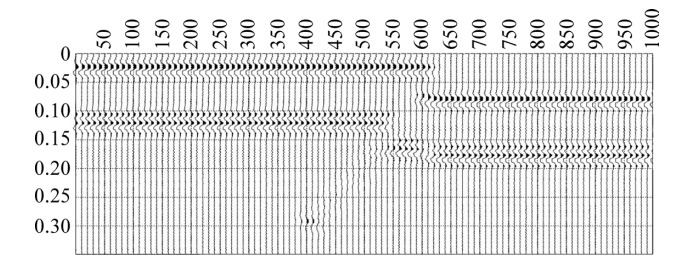


Figure 3: Seismic Forward Results of Fault Model

of 1,000m. The seismic forward is performed using the Tesseral software.

Figure 3 is a seismic cross-sectional view from the fault forward, and the displacement of the position is clearly seen at about the 600m in the lateral direction. In the heading side of the fault, the interface between the positions is found to be bent near the fault, mainly because the wave velocity of the fracture zone is smaller than that of the surrounding rock.

Figure 4 shows the inversion results of the fault model. GeoView software is used for inversion, in which the abscissa is the CDP point number, the ordinate is the time in milliseconds, and the red curve in the lateral 70 is the density logging curve. In the lateral direction 61 and vertical 30ms, a significant dislocation of the position occurs, which takes place in the upper position of the fault. The fluctuation of the position between lateral 55-65 and vertical 30-200ms is mainly because the wave velocity of the fault fracture zone is small. While in the lowest part, there is a clear inclined interface, which is the interface of the

fault fracture zone. There is a great difference between the setting of the fracture zone and the surrounding rock in this forward, thus the obvious fault fracture zone to be seen. However, the general response of the fracture zone is not so clear.

3.2 Forward of Transient Electromagnetic Method

Figure 5 shows the forward model established by the numerical simulation of the TEM. The model is the same size as the seismic forward model, with the aquosity of the fault considered and the parameters shown in the following figure. The transmitting coil is a rectangular $600*600m^2$ transmitting coil, and the transmitting current is 5A. The center loop device is used for collection, and the measuring point spacing is 20m, with 51 measuring points in total. The fault fracture zone has a conductivity of 0.1S/M and a width of 20m. Except for the overburden, the fault penetrates through all the underlying positions.

Figure 6 is a multi-channel profile from the transient electromagnetic forward. In the figure, the blue measuring point curve is the measuring channel of the early part, while the red measuring point curve is the curve of the later part. The response value of the left measuring point of the early multi-channel curve is higher than the right measuring point. The left side of the late multi-channel curve is lower than the right side, mainly because the left overburden is thinner in the model, and the resistivity of the underlying stratum is relatively high. Moreover, the early

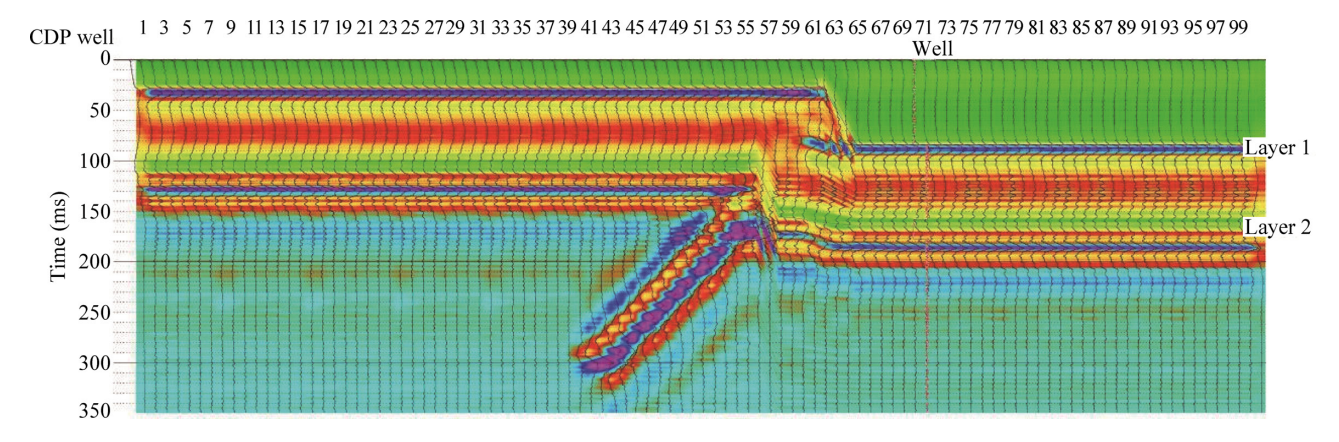


Figure 4: Seismic Wave Impedance Inversion Results of Fault Model

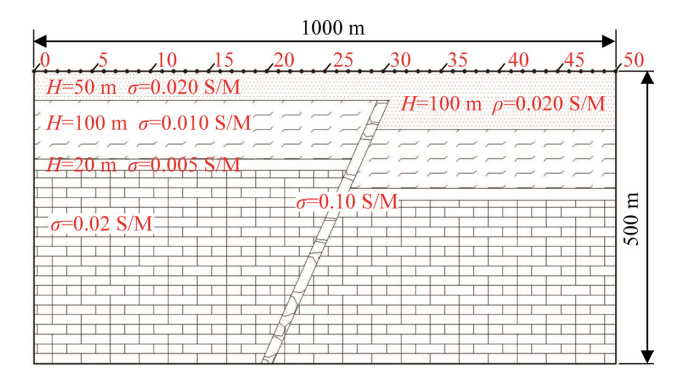


Figure 5: Forward Model of TEM

and late multi-channel curves show obvious downward and upward bending, respectively at lateral –200m and 200m, because the device is in the form of a center loop device in simulation, and the fault fracture zone has a relatively low resistivity. When the edge of the transmitting coil is close to the position of the fault, the density of the magnetic flux line passing through the fault fracture zone becomes larger, which has a greater influence on the observed data. Meanwhile, the value of the observed data is affected by the distance between the observed point and the abnormality. The smaller the distance, the greater the observation value being affected by the fault fracture zone.

3.3 Comprehensive Explanation

Figure 7 is the fault geoelectric model based on inversion results. The model length is 1,000m and the width is 500m. A drilling data is set for 70 in CDP. The resistivity setting at the fault fracture zone is consistent with that of the surrounding rock, due to the uncertainty of the water-bearing

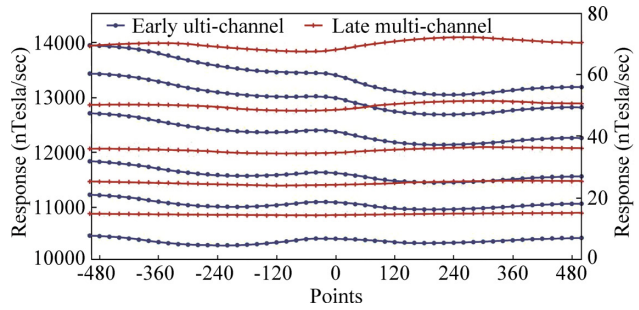


Figure 6: Multi-channel Profile of Fault Model of TEM

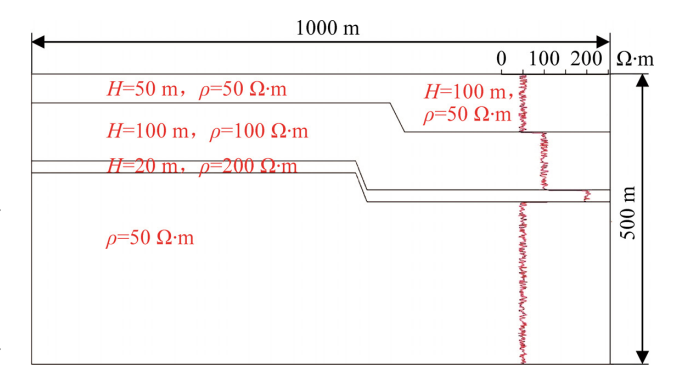


Figure 7: Fault Geoelectric Model Based on Inversion Results

capacity at the fracture zone, and the resistivity values of each layer being assigned according to the drilling data.

The transient electromagnetic forward calculation is performed for the geoelectric model shown above [16]. Figure 8 is a multi-channel profile, which formulated based on the forward calculation results. It can be seen from the figure that the induced electromotive force gradually decreasing from left to right in the early stage of the multichannel curve, while the induced electromotive force gradually shows an increase from the left to right in the later stage. These mainly because of the left low-impedance overburden being relatively thin, and the resistivity of the

576 — L. Yaoning et al. DE GRUYTER

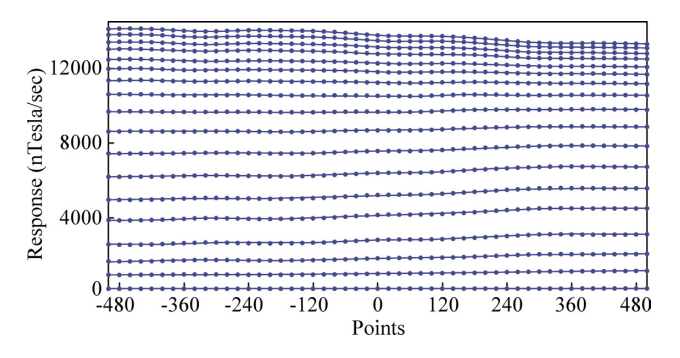


Figure 8: Multi-channel Profile

underlying layer is relatively high, which has similar results to those in Figure 6.

The difference between the transient electromagnetic forward result is shown after the comprehensive interpretation is analyzed. Figure 9 shows the position where the black line of the multi-channel profile of the induced electromotive force is 0 scale mark after the difference. In the early stage, the response value obtained by the transient electromagnetic forward based on the original model is smaller than that obtained by the forward based on the seismic wave impedance inversion model, indicating a negative response after the difference. In the later stage, the response is larger and positive after the difference, because the fault model set during the transient electromagnetic forward is a relatively low-impedance model, and the early response value of attenuation is relatively small. The fault aguosity can still be discriminated in the case of a relatively low resistivity of the overburden. Moreover, the multi-channel curve has different peak points, where the left peak is smaller than the right peak at lateral of -120m and 120m, mainly because that the fault model is set to the inclined state, and the right end of the fault being buried shallowly, while the left side is buried deeply. The influence of the fault on the ground response signal is that the left side is weaker than the right side. According to the peak point and position, the tendency and extension of the fault can be discriminated.

4 Instance Analysis

In order to verify the feasibility of the transient electromagnetic interpretation method based on the seismic inversion model in a practical observation, we combine the previous three-dimensional seismic exploration data of a certain work area for a comprehensive explanation on the transient electromagnetic exploration results.

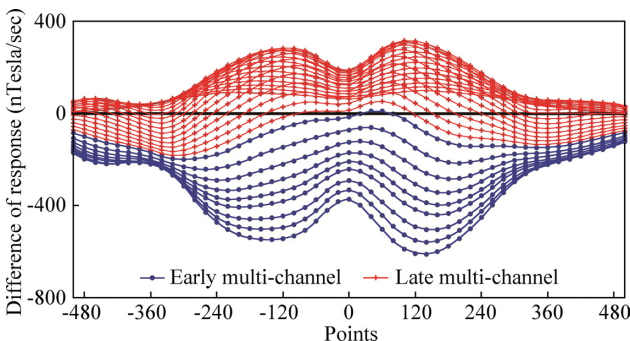


Figure 9: Multi-channel Profile

The #1 well logs was selected for inversion, and the seismic data is hierarchically constrained by the #1 well logs data to obtain the wave impedance inversion results in the following figure, in which the GDP dot spacing showing 5m. As shown in Figure 10, the position dislocation occurs at the lateral 22 and the vertical 200ms based on the previous seismic exploration data, and it was determined that the position is a fault. According to the overlying GDP number, the total length of the line is 500m. According to the known well logs curve, the maximum depth of the position divided is 450m.

The seismic inversion results are combined with the resistivity logging data to establish a geoelectric model. As shown in Figure 11 (a), the left curve is the density well logs, while the right curve is the resistivity well logs. According to the figure, the resistivity change is not too large in the area where the density of the rock ore changes greatly, while the density change is relatively flat in the area where the resistivity change is relatively obvious. The ground potential model of the resistivity related to the position is established, thus the wave impedance inversion is performed according to the density logging data during the position division to determine the position fluctuation, and the different position resistivity is divided according to the resistivity logging curve, with the modeling shown in Figure 11 (b).

Figure 12 is a multi-channel profile from the established geoelectric model for a transient electromagnetic forward. According to the figure, the response value increases significantly at the position between lateral 4 and 5, while the response value does not change as much as that in other positions, mainly because the established geoelectric model is a fault model with a dislocation in the lower stratum at point 4 and 5.

Figure 13 is a sectional view of apparent resistivity of the geoelectric model forward calculation. The apparent resistivity increases gradually with the increase of depth, which is similar to the results of the sectional view of the

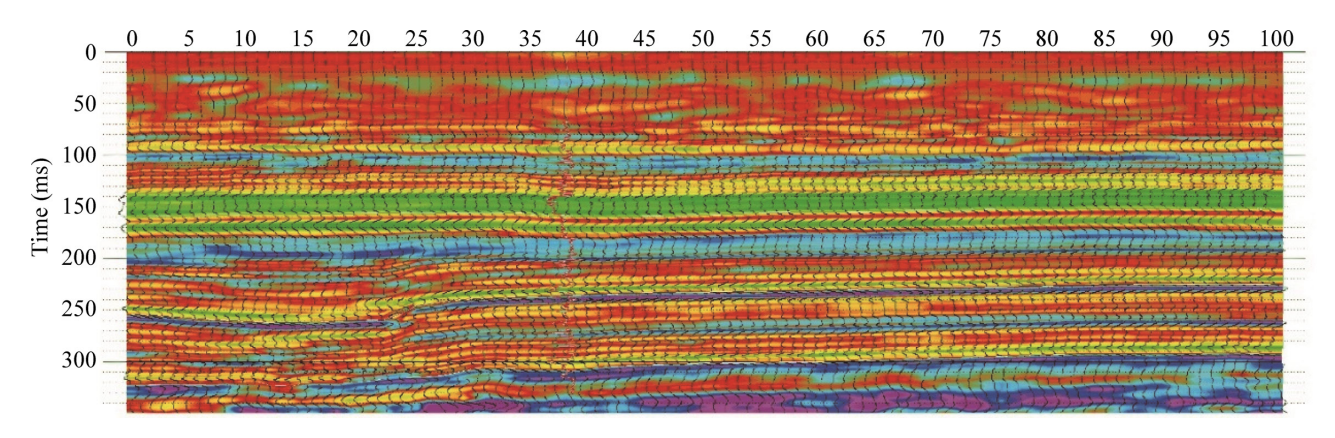


Figure 10: Seismic Wave Impedance Inversion Results

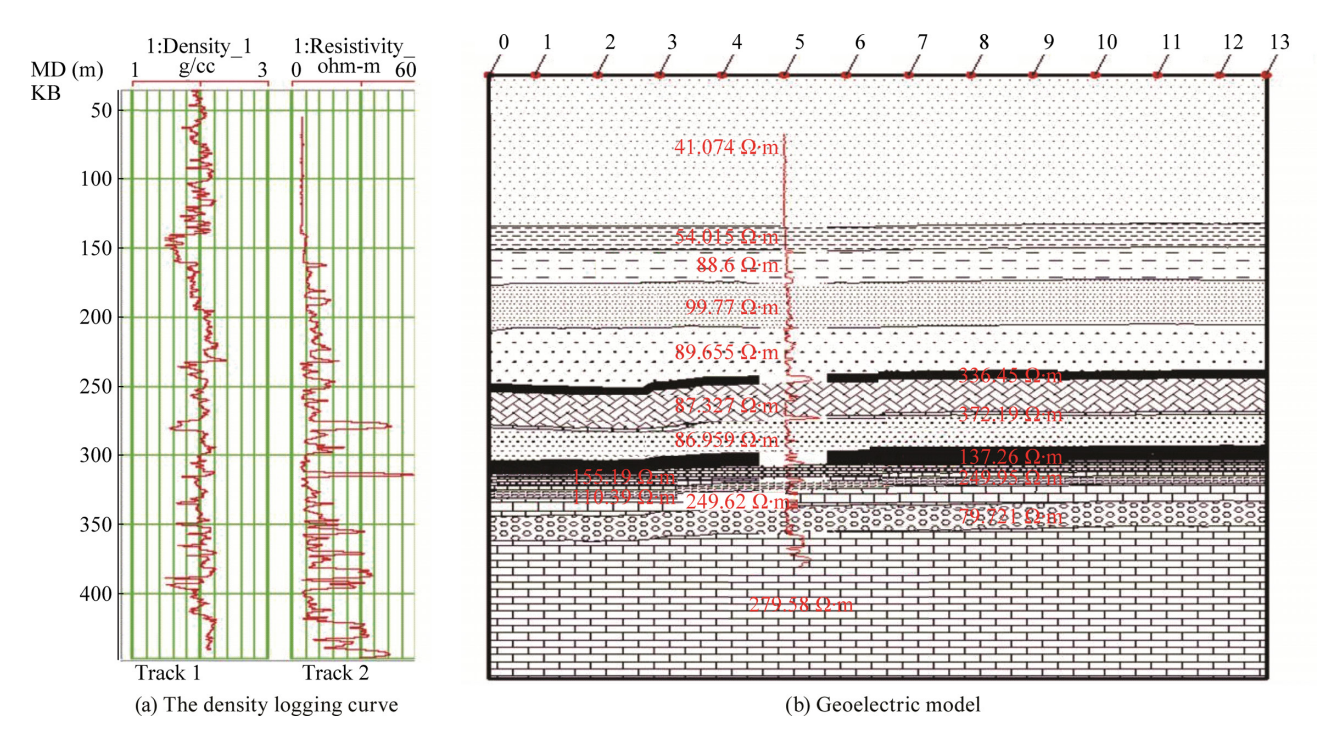


Figure 11: Establishment of Geoelectric Model

measured apparent resistivity, indicating that the establishment of the model is similar to the actual situation. According to the figure, the resistivity position jumps slightly, and the apparent resistivity increases gradually with the increase of the apparent depth, mainly because the resistivity tends to increase when the depth increases as the model is established.

Figure 14 is a multi-channel profile of the measured data. The induced electromotive force jumps between the points 4 and 5. In the late stage, the induced electromotive force jumps at points 10-13, and the multi-channel curve appears to be intersected. Therefore, the measured data quality at this position is poor.

Figure 15 is a sectional view of an apparent resistivity of the measured data after the apparent resistivity calculation and the apparent depth conversion. There is an obvious high-resistance at the horizontal 350 to 500m and the vertical –350 to –700m. Combined with the multi-channel data, it can be found that the data jumps at this position, which is caused by the poor data quality. Combined with the seismic inversion results, it can be seen that the position of the underground fault is at the horizontal 100-150 m. According to Figure 15, the fault and the surrounding parts are shown as a high impedance, which is initially judged as a non-conducting water-bearing fault.

Figure 16 is the result of a comprehensive interpretation, that is, the apparent resistivity calculated from the 578 — L. Yaoning et al. DE GRUYTER

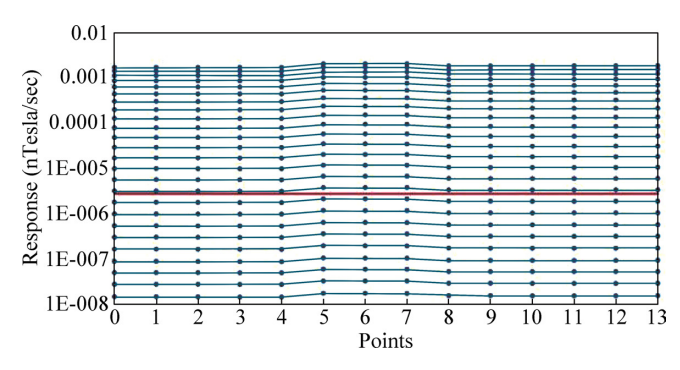


Figure 12: Multi-channel Profile of Geoelectric Model

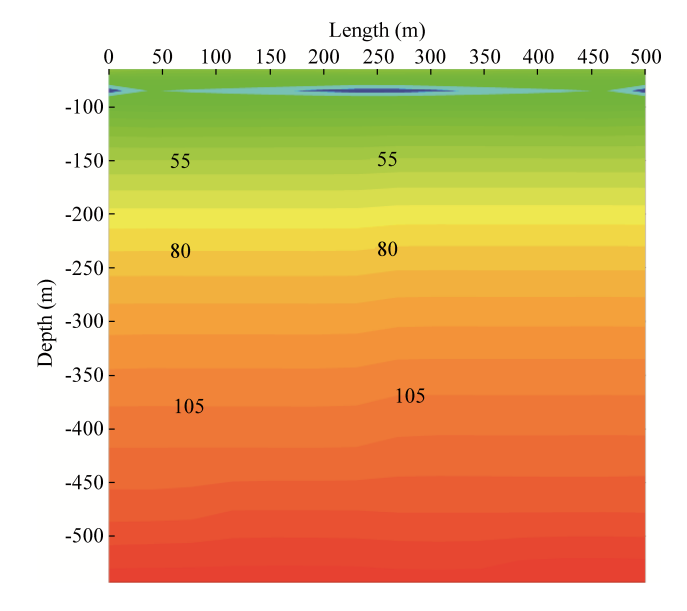


Figure 13: Sectional View of Apparent resistivity of Geoelectric Model

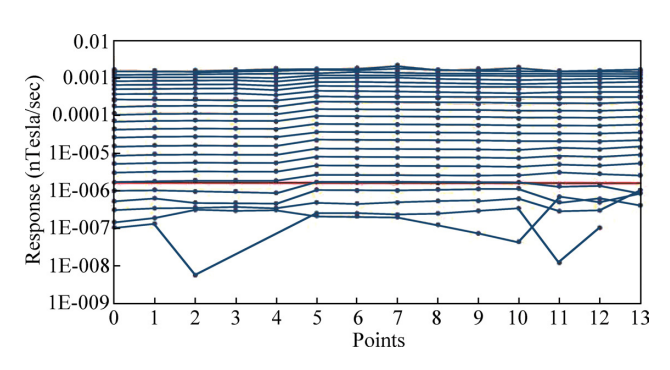


Figure 14: Multi-channel Profile of Measured Data

measured data minus the apparent resistivity calculated from the established geoelectric model. The difference at the vertical of –100m is small, indicating that the lateral change of resistivity in the shallower depth range is not much different from the logging resistivity value, which is affected by the Quaternary low-impedance stratum. At the lateral of 350 to 500m and the vertical of -430 to -540 m,

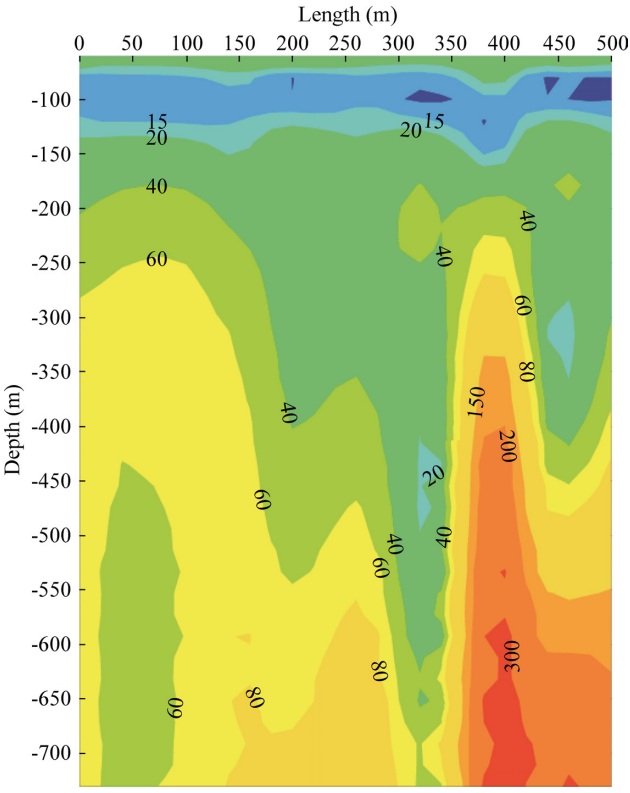


Figure 15: Sectional View of Apparent resistivity of Measured Data

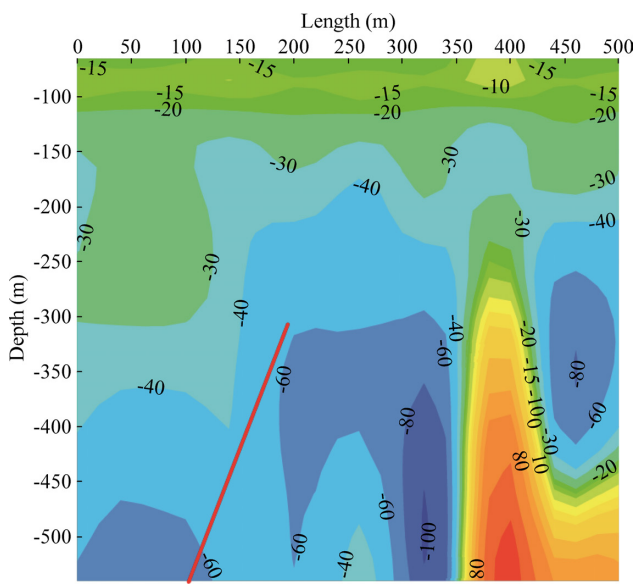


Figure 16: Sectional View of Apparent Resistivity Difference

there are larger positive values, which are mainly caused by the interference of the measured data of the transient electromagnetic and cannot be avoided. At the lateral 0 to 350m and the vertical –200 to –540 m, there are larger negative values, indicating that the stratum resistivity in this range is smaller than the logging resistivity. The red diag-

onal line drawn in the figure represents the fault location and direction. It can be found that the difference between the resistivity at the fault location is larger than the absolute value of the difference between the resistivity of the surrounding rock. Thus can be judged that the resistivity at the fault location is lower than that of the surrounding rock, and the fault of this position is conducting and water-bearing through verification.

5 Conclusions

The interpretation method of the transient electromagnetic based on the seismic wave impedance inversion model is studied in detail in this paper, with the following conclusions obtained:

- (1) This paper proposes a comprehensive interpretation method of transient electromagnetic based on wave impedance inversion for the problems existing in the interpretation of current geophysical exploration data and introduces the flow of the explanation method in detail.
- (2) The typical geophysical model with faults is selected to verify the interpretation method based on forward modeling data. According to the study, this interpretation method can effectively avoid the influence of low-impedance overburden on data interpretation. The positive and negative values and the peak value of the data after the difference analysis are possible to judge not only the water-bearing property of the fault but also the fault tendency.
- (3) The interpretation method is verified based on an example. The position and conducting aquosity of the work area structure are accurately explained. Through the sectional view of apparent resistivity difference, the influence of the shallow lowimpedance stratum is eliminated, which better highlights the structure and the electrical variation characteristics of the stratum.

Acknowledgement: This study is funded by "the National Key R&D Program of China (Grant NO.2018YFC0807802-3)" and "A Project Funded by the Priority Academic Program Development of Jiangsu Higher Education Institutions (PAPD)".

References

- [1] Danielsen J E., Auken E., Jørgensen F., The application of the transient electromagnetic method in hydrogeophysical surveys. Journal of Applied Geophysics, 2003, 53(4), 181-198, DOI:10.1016/j.jappgeo.2003.08.004
- [2] Liu S-C., Liu X-M., Characteristics of apparent resistivity with the electrical changing of water conducted structures under the mining-induced effect. Journal of Mining and Safety Engineering, 2010, 27(03), 316-321.
- [3] Wang R., Yin C., Wang M., Laterally constrained inversion for CSAMT data interpretation. Journal of Applied Geophysics, 2015, 121(7), 63-70, DOI:10.1016/j.jappgeo.2015.07.009
- [4] Chang J-H., Yu J-C., Liu Z-X., Three-dimensional numerical modeling of full-space transient electromagnetic responses of water in goaf. Applied Geophysics, 2016, 03), 539-552, DOI: 10.1007/s11770-016-0572-y
- [5] Yue J-H., Xue G-Q., Review on the development of Chinese coal electric and electromagnetic prospecting during past 36 years. Progress in Geophysics (in Chinese), 2016, 31(4):1716-1724, DOI: 10.6038/pg20160441.
- [6] Xue G-Q., Yu J-C., New development of TEM research and application in coal mine exploration. Progress in Geophysics (in Chinese), 2017, 32(1): 0319-0326, DOI: 10.6038 /pg20170145
- [7] Zhao L-M., Cui R-F., Application of digital high-density seismic exploration in fine structural interpretation in coalfield. Progress in Geophysics (in Chinese), 2014, 29(5):2332-2336, DOI: 10.6038/pg20140551.
- Zhao X-Z., Zhang W., Deng Z-W., 2.5 times 3D seismic exploration method for complex geological targets. Oil Geophysical Prospecting, 2014, 1039-1047+1.
- [9] Li T-L., Zhang R-Z., Pak Y-C., Joint inversion of magnetotelluric and first-arrival wave seismic travel time with cross-gradient constraints. Journal of Jilin University: Earth Science Edition, 2015, 45(3):952-961, DOI:10.13278/j.cnki.jjuese.201503304.
- [10] Cheng J-Y., Zhao W., Cao D-T., Wang Tieji., Pondering on coalmine winning district 3D seismic correlation of prospecting and mining information effect analysis. Coal geology of China, 2010, 22 (08), 67-72+82, DOI: 10.3969/j.issn.1674-1803.2010.08.17
- [11] Wei S-H., Wang J-Q., Discussion on the accuracy evaluation standard of structural interpretation results of three-dimensional seismic exploration in coalfield. China mining magazine, 2018, 07, 135-138, DOI:10.12075/i.issn.1004-4051.2018.07.008.
- [12] Wang X-H., Xiong Y-J., Wu H-L., Talking about the Development Status of Coal Geophysical Technology. West-china Exploration Engineering, 2017, 07), 135-136+140.
- [13] Li H., Fan Y-R., Hu Y-Y., Zheng S-G., Sun Q-T., Joint inversion of HDIL and SP with a five-parameter model for estimation of connate water resistivity., Chinese Journal of Geophysics. (in Chinese), 2013, 56(2):688-695, DOI:10.6038/cjg20130233.
- [14] Li Q., Peng S., Zou G., High resolution processing of 3D seismic data for thin coal seam in Guqiao coal mine: Journal of Applied Geophysics, 2015, 115(32-39), DOI:10.1016/j.jappgeo.2015.02.014
- [15] Liu Y., Lu Q-T., Meng G-X., Yan J-Y., Zhang K., Yang Z-W., Joint electromagnetic and seismic inversion survey: status and prospect. Progress in Geophysics (in Chinese), 2012, 27(06), 2444-2451, DOI:10.6038/j.issn.1004-2903.2012.06.019.

[16] Li J-H., Zhu Z-Q., Liu S-C., Liu X-M., Zeng S-H., Luo W-X., Rectangular loop transient electromagnetic field expressed by G-S algorithm. OGO, 2011, 46(3); 489-492.